NEW METHOD TO DETERMINE TENSION SOFTENING CURVE OF CONCRETE

J. Niwa,
Department of Civil Engineering, Tokyo Institute of Technology,
Tokyo, Japan
T. Sumranwanich,
School of Civil Engineering, Asian Institute of Technology,
Bangkok, Thailand
S. Tangtermsirikul,
Sirindhorn International Institute of Technology, Thammasat University,
Bangkok, Thailand

Abstract
A new method to determine the tension softening curve of concrete has been proposed. To solve the problems included in the modified J-integral based method, the release of elastic energy has been considered quantitatively. In addition, the propagation of the fictitious crack has been evaluated quantitatively. The new method in which these new findings are incorporated has been applied to estimate the tension softening curve of various types of concrete, and the validity of this method has been confirmed experimentally.
Key words: Tension softening curve, J-integral based method, fictitious crack, elastic energy

1 Introduction

Methods in current use for determining the tension softening curve of concrete are divided into two groups: (1) a numerical analysis method through inverse analysis, and (2) the J-integral based method based on energy balance. However, to date, no standard test method has been established to determine the tension softening curve.

Starting with the J-integral based method by Li, et al. (1989), a series of methods based on energy balance have been proposed: the new J-integral based method, Rokugo et al. (1989a), and the modified J-integral based method, Uchida et al. (1991). It has been pointed out that these methods have problems regarding the accuracy of measured data and the validity of assumptions used. However, with the understanding of the fracture phenomenon of concrete, these methods can help to improve the accuracy of estimation of the tension softening curve.

In this study, the release of elastic energy when energy is consumed, and the propagation of the fictitious crack in the ligament portion are highlighted and evaluated to propose an accurate method of determining the tension softening curve.

2 Problem of modified J-integral based method

In the modified J-integral based method, Uchida et al. (1991), the assumption regarding the distribution of the fictitious crack width has been improved. The fictitious crack is not uniformly distributed, but the crack is assumed to be distributed as if it were rotating around an axis at the flexural compression fiber of a notched beam.

However, the following assumptions still remain unchanged in the modified J-integral based method: (a) the assumption that external energy applied to a specimen is completely consumed in the fictitious crack; and (b) the assumption that the fictitious crack propagates throughout the ligament portion immediately after loading.

If these assumptions are changed to be more realistic ones, the tension softening curve will be more accurately evaluated. Therefore, in this study these two points are examined and improved.

3 Release of elastic energy

3.1 Outline
In the modified J-integral based method, the consumed energy $E(\omega)$ is calculated as the right hand side of Eq.(1). However, it is actually the potential energy (Fig. 1).

$$E(\omega) = \int_0^{\delta_w} P(\delta)\, d\delta \tag{1}$$

where, ω is the fictitious crack width, and δ_w is the displacement of a notched beam corresponding to the crack mouth opening, w.
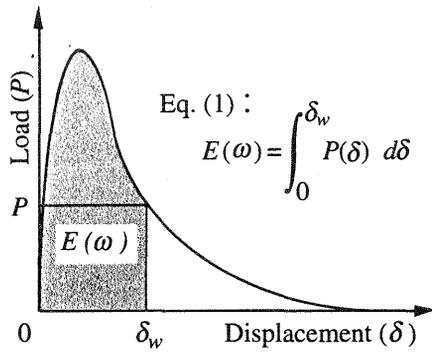
Fig. 1. Energy in Eq. (1)

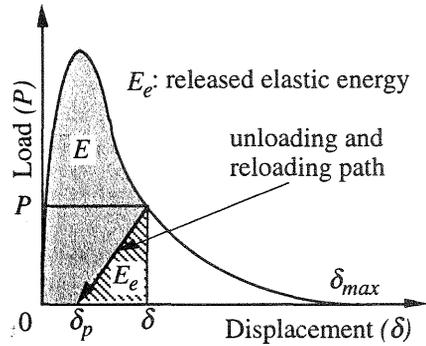$$E(\omega) = \int_0^{\delta_w} P(\delta)\, d\delta$$

Fig. 2. Release of elastic energy

In the modified J-integral based method, this energy is assumed to completely be consumed in the fictitious crack. However, a part of the external energy accumulates in other portions besides the fictitious crack, and the energy must be released as elastic energy during the unloading process as shown in Fig. 2. Therefore, to properly evaluate the energy consumed in the fictitious crack, the amount of elastic energy released must be excluded. In this study, unloading and reloading path was determined by test results, and based on this, released elastic energy was quantitatively evaluated.

3.2 Unloading and reloading tests for a notched beam

If the unloading and reloading path can be assumed to be linear, Eq. (1) can be rewritten as Eq. (2).

$$E(\omega) = \int_0^{\delta} P(\delta)\, d\delta - \frac{1}{2} P(\delta)(\delta - \delta_p) \tag{2}$$

where, δ_p is the residual displacement in a fully unloaded state.

To formulate δ_p in Eq. (2), the unloading and reloading operation in

Table 1. Mix proportion of concrete

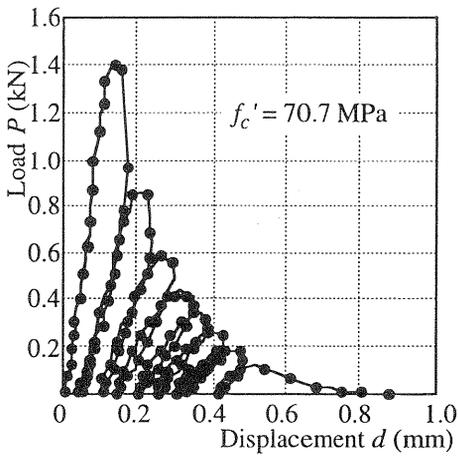| Type of concrete	W/B (%)	s/a (%)	Unit weight (kg/m^3)							
			W	C	Fly ash	Silica fume	Fine aggregate	Coarse aggregate	Admixture (%)	Air (%)
Self-compacting	24	58	159	530	133	—	896	664	2.2	2.0
High strength	22	42	116	488	—	37	768	1084	2.4	1.0
Normal strength	60	45	190	316	—	—	819	1024	—	1.0

Fig. 3. Load-displacement relation
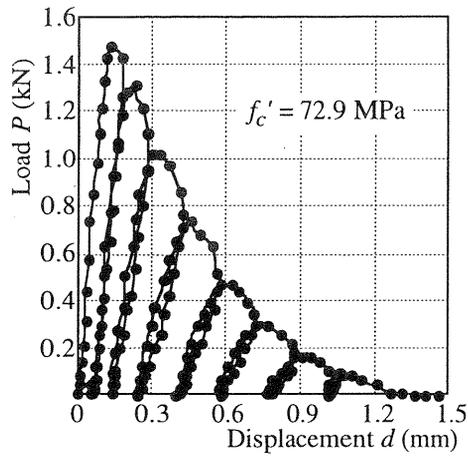(Self-compacting concrete, 28 days)

Fig. 4. Load-displacement relation
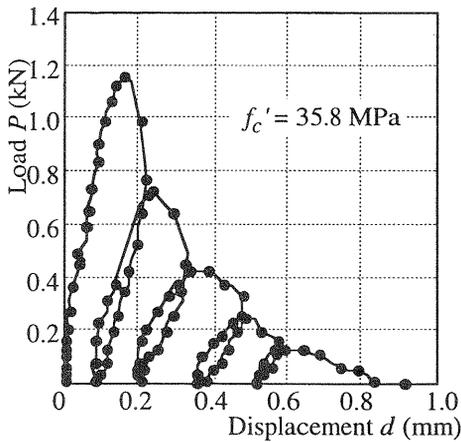(High strength concrete, 3 days)

Fig. 5. Load-displacement relation
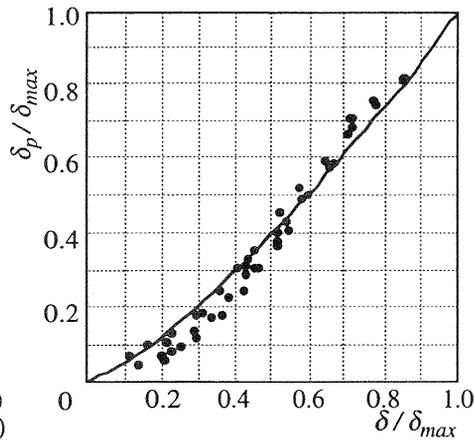(Normal strength concrete, 28 days)

Fig. 6. δ_p/δ_{max} and δ/δ_{max} relation

the post-peak region has been repeated for a simply supported notched beam specimen (width 100 mm × height 100 mm × length 840 mm, span 800 mm, notch depth 50 mm). Three types of concrete were used as shown in Table 1. Figs. 3 - 5 show the measured load-displacement relations for self-compacting concrete, high strength concrete, and normal strength concrete, respectively.

The maximum displacement (= the final displacement) on the load-displacement curve is δ_{max}, unloading displacement is δ, and residual displacement under fully unloaded states is δ_p; δ and δ_p are corrected for

350

δ_{max} for all test data, and the relations between δ_p/δ_{max} and δ/δ_{max} are plotted as shown in Fig. 6.

Further, δ_p/δ_{max} is indicated as an exponent of δ/δ_{max}, shown in Fig. 6 as a solid curve. This relation is indicated by Eq. (3).

$$\frac{\delta_p}{\delta_{max}} = \left(\frac{\delta}{\delta_{max}}\right)^{1.38} \tag{3}$$

In this study, the portion of elastic energy released was evaluated using Eq. (3).

4 Evaluation of propagation of the fictitious crack

4.1 Measurement of the fictitious crack width

It is only an assumption that the fictitious crack propagates throughout the ligament area immediately after the loading. Actually, it must gradually propagate as the displacement increases. As indicated in Fig. 7, when the ligament length is a_o, the fictitious crack length is "a", and the fictitious crack width is $\omega(y)$, the following relation can be obtained.

$$\omega(y) = w\,y\,/\,a$$
$$y = a\,\omega(y)\,/\,w$$
$$dy = (a\,/w)\,d\omega \tag{4}$$

Then, the energy E which is consumed in this portion can be calculated as follows:

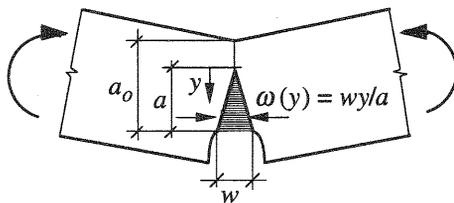$$E = b \int_0^w e(\omega)\frac{a}{w}\,d\omega = \frac{b\,a}{w}\int_0^w e(\omega)\,d\omega \tag{5}$$

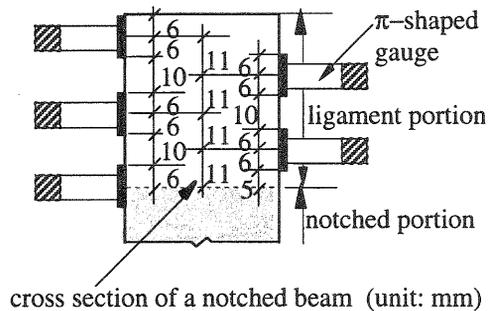Fig. 7. Propagation of a fictitious crack

Fig. 8. Arrangement of π-shaped gauges

From Eq. (5), the tension softening curve can be derived.

$$\int_0^w e(\omega) \ d\omega = \frac{w}{b \, a} E(w)$$

$$e(w) = \frac{1}{b \, a}\left[E(w) + w \, E'(w)\right]$$

$$\sigma(w) = \frac{de(w)}{dw} = \frac{1}{b \, a}\left[2 \, E'(w) + w \, E''(w)\right] \tag{6}$$

This is the tension softening curve. Eq. (6) is different from the modified J-integral based method because the softening stress $\sigma(w)$ is dependent on the fictitious crack length a.

To evaluate the propagation of the fictitious crack in the ligament portion, the longitudinal strain distribution of a notched beam has been measured. π-shaped gauges (base length is 100 mm) were provided in the ligament portion of a notched beam. For the purpose of obtaining as much measured data as possible to evaluate the fictitious crack propagation, five π-shaped gauges (three on one side, two on the other side) were placed on the 50-mm high ligament portion. Each π-shaped gauge was set 11 mm apart as shown in Fig. 8.

The outputs from the five π-shaped gauges disposed at the ligament portion are assumed to be the fictitious crack width, and the distribution is plotted in Fig. 9. Strictly speaking, this fictitious crack width includes the elastic deformation in this portion. The elastic stress generated in this
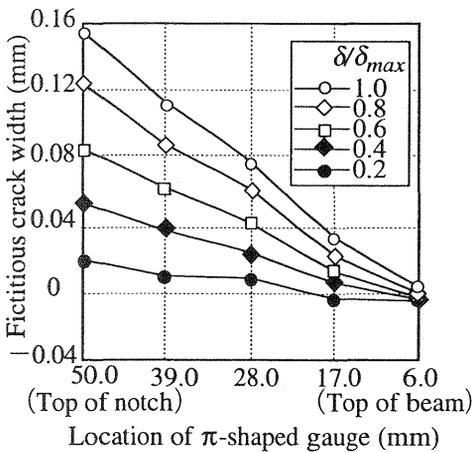
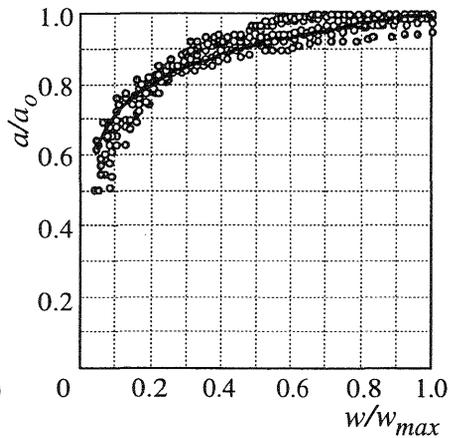Fig. 9. Distribution of fictitious crack width (Self-compacting concrete, 28 days)

Fig. 10. Fictitious crack length and crack mouth opening relation

352

portion is less than the level of the tensile strength of concrete; therefore, the elastic deformation is also evaluated as being below about 0.01 mm, which is judged to be negligible in comparison with the fictitious crack width, so we can assume that the measured data corresponds to the fictitious crack width.

As shown in Fig. 9, a clear compression zone can be observed near the upper edge of the beam when δ/δ_{max} is 0.2 or 0.4, and it has been confirmed that the fictitious crack does not reach to the top. However, the compression zone narrows as the displacement increases, and when δ/δ_{max} becomes 0.8, the fictitious crack has propagated throughout the ligament portion.

4.2 Evaluation of the fictitious crack propagation

If the behavior of fictitious crack propagation is indicated as a function of, for example, relative displacement δ/δ_{max} or relative crack mouth opening w/w_{max}, it becomes possible to quantitatively deal with the fictitious crack propagation. In Fig. 10, the relative fictitious crack length a/a_o, obtained by dividing the fictitious crack length "a" (corresponding to the point at which the fictitious crack width is zero in Fig. 9), by the ligament length a_o is plotted in relation with w/w_{max}.

As shown in Fig. 10, while the crack mouth opening is small during the initial stage after loading, the fictitious crack length remains between 50% and 80% of the ligament length. On the other hand, as loading proceeds, the fictitious crack propagates to the upper edge of the beam, and when w/w_{max} becomes about 50%, a/a_o becomes about 90% or more. The solid curve in Fig. 10 is derived from plotted data and given by Eq. (7).

$$\frac{a}{a_o} = 1.0 + 0.125 \, ln \left(\frac{w}{w_{max}} \right) \tag{7}$$

where, $0.05 \leqq w/w_{max} \leqq 1.0$.

In this study, the propagation of the fictitious crack was evaluated using Eq. (7).

5 Comparison of tension softening curves

5.1 Material property of concrete

Compressive strength f_c', tensile strength f_t, and fracture energy G_F of three types of concrete in this study are shown in Table 2.

5.2 Tension softening curve of concrete

In order to confirm the validity of the proposed method, the tension softening curves obtained by the modified J-integral based method and

Table 2. Material properties of concrete

Age	1 day			3 days			28 days		
Type of concrete	f_c' MPa	f_t MPa	G_F N/mm	f_c' MPa	f_t MPa	G_F N/mm	f_c' MPa	f_t MPa	G_F N/mm
Self-compacting	34.6	3.33	0.10	46.8	4.41	0.13	70.7	5.68	0.15
High strength	58.5	5.10	0.11	72.9	5.59	0.14	94.7	5.78	0.15
Normal strength	13.1	1.57	0.09	25.0	2.74	0.09	35.8	3.72	0.11

the proposed method are compared.

In each method, the estimated value of initial softening stress does not completely coincide with the tensile strength of concrete obtained through the splitting test. Therefore, the initial softening stress was replaced by the tensile strength of concrete.

Figs. 11 - 13 show tension softening curves for self-compacting concrete, high-strength concrete, and normal strength concrete, respectively. In each figure, the tension softening curves estimated by the modified J-integral based method and the proposed method are shown; the broken lines indicate tension softening curves according to the 1/4 model, Rokugo et al. (1989b). Since the 1/4 model is known as its high conformity with test data, it is considered to be a typical example of tension softening curves.
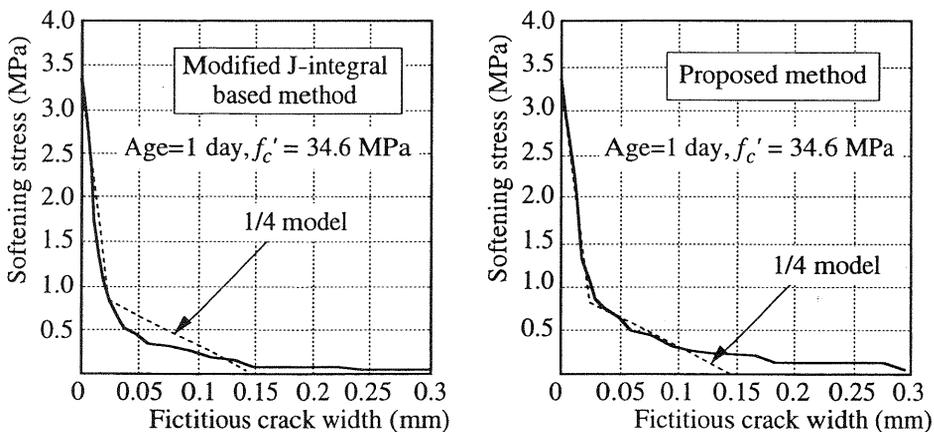
From Figs. 11 - 13, the following can be observed.

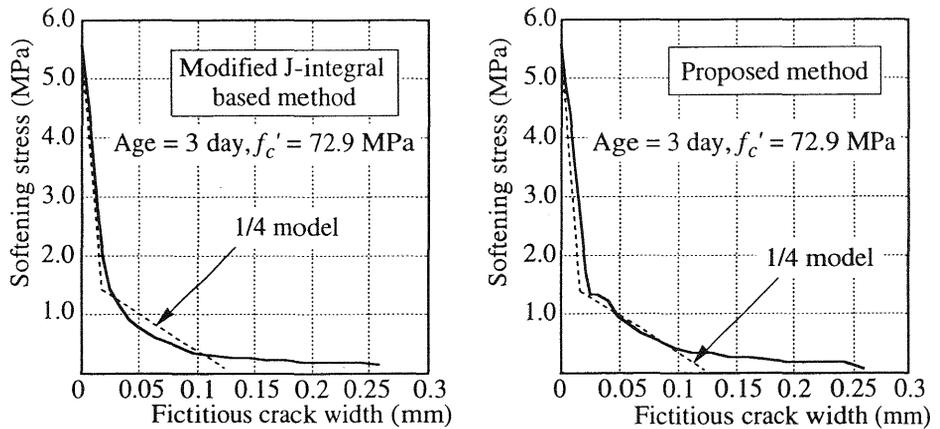Fig. 11. Tension softening curve of self-compacting concrete

354

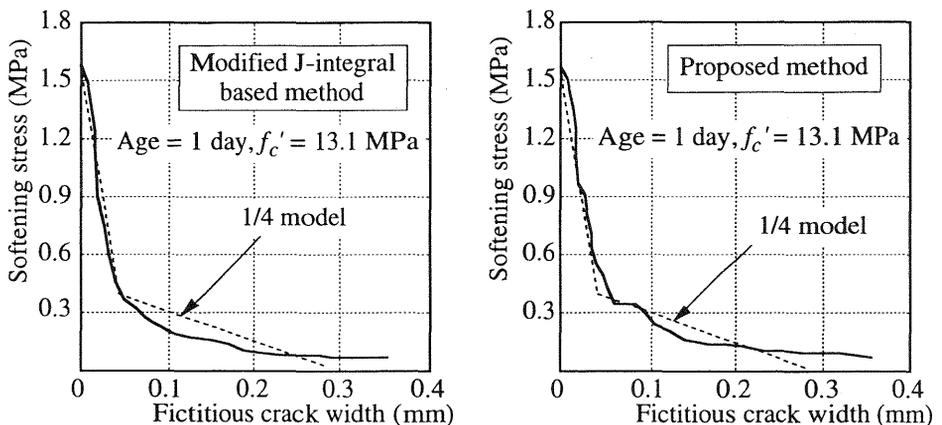Fig. 12. Tension softening curve of high strength concrete

Fig. 13. Tension softening curve of normal strength concrete

The tension softening curves obtained by the modified J-integral based method are considerably smooth for each type of concrete. Further, a long tail portion, where the stress gradually decreases as the fictitious crack width increases, can also be estimated. Therefore, as a method of estimating the tension softening curve, this method seems fairly satisfactory. However, close examination, for instance, for the gradually inclined portion of the tension softening curve (corresponding to the second inclined portion of the 1/4 model), indicates some difference between the modified J-integral based method and the 1/4 model, so there is some room for improvement.

The tension softening curve obtained by the proposed method, in which the modified J-integral based method is further modified by the two points, is slightly lacking in the smoothness when compared to that

obtained by the modified J-integral based method, but the difference in the gradually inclined portion is considerably improved. In addition, the long tail portion of the tension softening curve can also be estimated.

With the proposed method, it may be possible to estimate a tension softening curve resembling that of the 1/4 model regardless of the type of concrete. It means the validity of the proposed method.

6 Conclusion

The modified J-integral based method was improved by evaluating the release of elastic energy and the propagation of the fictitious crack in the ligament portion. In order to consider the portion of elastic energy released, unloading and reloading tests for notched beams were carried out in the post-peak region, and the residual displacement was quantitatively formulated. Further, the propagation of the fictitious crack was quantitatively evaluated based on the measurement of the fictitious crack length by π-shaped gauges.

The tension softening curve obtained by the proposed method, in which above two points of the modified J-integral based method were further improved, is somewhat lacking in the smoothness when compared to that obtained by the modified J-integral based method. However, it is superior to that obtained by the modified J-integral based method because it has the excellent conformity with the 1/4 model, considered to be the typical tension softening curve of concrete.

7 References

Li, V.C. and Ward, R.J. (1989) A novel testing technique for post-peak tensile behavior of cementitious materials, in **Fracture Toughness and Fracture Energy**, Balkema, 183-195.

Rokugo, K., Iwasa, M., Seko, S. and Koyanagi, W. (1989a) Tension softening diagrams of steel fiber reinforced concrete, in **Fracture of Concrete and Rock**, Elsevier, 513-522.

Rokugo, K., Iwasa, M., Suzuki, T. and Koyanagi, W. (1989b) Testing method to determine tensile strain softening curve and fracture energy of concrete, in **Fracture Toughness and Fracture Energy**, Balkema, 153-163.

Uchida, Y., Rokugo, K. and Koyanagi, W. (1991) Determination of tension softening diagrams of concrete by means of bending tests. **Journal of Materials, Concrete Structures and Pavements of JSCE**, No.426/ V-14, 203-212.